Qu, Y., et al., 2019, Evidence for molecular structural variations in the cytoarchitectures of a Jurassic plant: Geology, https://doi.org/10.1130/G45725.1

1. Geological background

The Mesozoic strata at the Korsaröd locality, north of Höör in southern Sweden, represents a 'Konservat-Lagerstätten' deposit, hosting well-preserved fossilized plant material from a terrestrial ecosystem, including spore, pollen, charcoal, wood fragments with growth rings and saprophytic fungi (McLoughlin and Bomfleru, 2016; Vajda et al., 2016). The Jurassic Korsaröd successions record episodic lahar events, which partially preserved the vegetation of the contemporaneous ecosystem. In remarkable cases, the rapid calcite-permineralization by hydrothermal brines during volcanism has well-preserved the plant cytoarchitectures (Bomfleur et al., 2014; Vajda et al., 2016). The age of the strata is constrained to the Early Jurassic 191-176.7±0.5 Ma, according to $^{40}Ar/^{39}Ar$ estimates from adjacent basanite and nephelinite plugs (Bergelin et al., 2011; Tappe et al., 2016).

2. Methods

Petrography and Raman Spectroscopy

The petrographic and Raman spectroscopic analyses were performed on c. 40 μm thick polished thin sections of the fossil *Osmunda*, by using a A Horiba-Jobin Labram 800 HR Raman spectrometer linked to an Olympus BX41 petrographic microscope at the Centre for Geobiology at University of Bergen, and a Renishaw InVia spectrometer linked to an Olympus BX61 confocal microscope at the Institut de Physique du Globe de Paris in Paris, respectively. For the Horiba-Jobin Labram 800 HR spectrometer the Ar-ion laser with the wavelength of 514 nm, went through a density filter (D=0.3), an aperture hole of 100 μm in diameter, a 100× objective, and finally in a 1–2 μm spot on the sample with the final power of c. 0.2 mW (measured with a Coherent Lasercheck Analyser). For the Renishaw InVia Raman spectrometer exactly the same settings were applied, using a 514 nm laser with a 0.2 mW final power on the sample surface. In order to avoid polishing artifacts and potential contamination on the surface, we focused the laser beam on the carbonaceous material underneath polished surface of thin section. The spectra were acquired randomly from various cellular organelles in the range of 150–2000 cm^{-1} using a running time of 2×10 seconds. Some areas were scanned by using an XY stage with spatial resolution of 1 μm per step to generate two-dimensional maps of Raman spectral parameters. For Raman hyperspectral mapping each point analysis consisted of a running time of 1×5 seconds. The final data were processed with the software 'Lab Spec version 5.58.25' and Matlab version 7.13.0.564. The spectra were subtracted with a linear baseline

from 1000 to 1800 cm^{-1} to remove the background fluorescence (Fig. 1D). The peak fitting were performed by peak deconvolution using a Gauss-Lorentzian function with 100 iteration per fit.

micro-Fourier Transform Infrared spectroscopy (FTIR)

The micro-FTIR analysis was performed on doubly polished wafers using an infrared microscope (Bruker Hyperion 3000) linked to a Bruker IFS66V FTIR spectrometer in transmission mode at Beamline D7 in the MAX-Lab ring of Maxlab in Lund, Sweden. The absorbance spectra were obtained by focusing the IR through a 15×15 μm^2 aperture on the targeted samples in the rock wafer on the CaF_2 window. Reference background IR spectrum for calibration were measured on the CaF_2 window before the measurement of every sample. The FTIR spectrum acquisition has been performed randomly from various cellular organelles. The spectra in the range from 500 to 7500 cm^{-1} were obtained by the integration of 256 scans, and processed with the software Lab Spec version 5.58.25 and Matlab version 7.13.0.564.

SIMS (Secondary Ion Mass Spectrometry)

The *in-situ* isotopic analyses of the extant and fossil ferns were performed by using a Cameca IMS 1280 (Secondary ion mass spectrometry) at the Swedish Museum of Natural History in Stockholm (NORDSIM Laboratory). Slices from the fossil Royal fern stem (rhizome) were cut from polished discs, whereas the fresh slices from the extant Royal fern rhizome were first soaked in Na_2SiO_3 and solidified

in the air (reaction: $Na_2SiO_3+CO_2=SiO_2+Na_2CO_3$). Both the fossil and the extant Royal fern samples were mounted together with a graphite standard of pyrolytic graphite ('C-pyr' which has $\delta^{13}C$ = –31 ‰ in VPDB) in epoxy, and subsequently polished and coated with a c. 30 nm gold layer to provide conductivity. A 20 kV impact energy Cs^+ beam was focused to a 5–10 μm spot, and meanwhile a low energy electron flooding gun was used to compensate for charge build-up. Measurements were made in high transmission transfer mode with simultaneous determination of the ^{12}C and ^{13}C signals in a Faraday cup and low-noise ion counting electron multiplier, respectively, the latter of which was operated at mass resolution of M/DM=6000 to separate $^{13}C^-$ from $^{12}C^1H^-$, and M/DM=12000 to separate $^{11}B^{16}O$ from $^{13}C^{14}N$ at mass 27. Measurements were performed randomly from various cellular organelles. Carbon isotopic data were calibrated using the graphite standard and are reported as ‰ deviation from VPDB. In order to avoid analytical artifacts, we excluded all sample data points with excessively low ^{12}C count rate (defined as ion counts per second) relative to that of the bracketing graphite standards. When all $\delta^{13}C_{org\text{-}SIMS}$ data are plotted against ^{12}C count ratio (^{12}C count rate sample/standard), anomalous points with strongly deviating $\delta^{13}C$ values are observed for count ratios lower than 0.07 (Fig. DR1). These points with low ^{12}C count ratio represent spots with a small fraction of total organic material, and have therefore been excluded from our interpretation. This cut off is arbitrary, but in the same range as used in other studies (e.g. Morag et al., 2016; Wacey et al., 2011).

Analysis of carbon isotopic composition of organic carbon from bulk samples

The carbon isotopic analyses on organic carbon in both fossil and extant Royal fern samples were carried out at the University of Bergen using an Elemental Analyser Continuous Flow Isotope Ratio Mass Spectrometry (EA-CF-IRMS: ThermoScientific Delta V Plus with Costech EA). The weathered surfaces of rock pieces were cut off to avoid potential contamination. The powdered samples from bulk rock were rinsed with (ethanol/dichloromethane = 1:9 volume ratio) to remove possible organic contamination during crushing before evaporated in room temperature. The powdered samples were used for carbon isotopic analysis on organic carbon, and decarbonated using 37% (volume ratio) HCl at 70˚C for 48 hours and subsequently rinsed three times by deionized water and dried at room temperature. The $\delta^{13}C$ of carbonate and organic matter are reported relative to the VPDB standard (Standard Deviation < 0.04 ‰), and the appropriate correction factors were applied.

3. Description of the morphological and ultrastructural variations of organic matter in various stages of cell cycle based on optical microscopic images and Raman maps.

During the interphase stage, the nucleolus (arrow in Fig. 1E) appears with a clear boundary in the nucleus, whereas the chromatin in the nuclear matrix is difficult to identify by optical microscopy (Fig. 1E). The Raman spectra show that the nucleolus is less structurally ordered (lower I-1350/1600) compared to the ambient nuclear matrix, which is well packed by the smooth nuclear envelope. In the prophase, the

nucleolus disintegrates, and the nuclear envelope starts to crack (Fig. 1J). The chromatin starts to convert into chromosomes, which distribute randomly in the nuclear matrix (Fig. 1J). The chromosomes contain higher concentration of organic carbon (higher I-1600) and higher structural order (higher I-1350/1600) than the nuclear matrix (Fig. 1J). In the prometaphase, the chromosomes continue concentrating in specific areas in the nucleus, where the structural order of carbon is slightly higher (higher I-1350/1600) than the nuclear matrix (Figs. 2K–L). In the metaphase, the condensed chromosomes gradually gather near the equator in the center of the nucleus (Fig. 1M) and the structural order of carbon is higher (higher I-1350/1600) in the chromosomes than that in the nuclear matrix (Fig. 1M). In the anaphase, the chromosomes/chromatids split and move towards the opposite sides (arrows) of the cell and display lower structural order (lower I-1350/1600) of carbon compared to the nuclear matrix (Fig. 1N). In the telophase, the cell plate forms in the center (dashed line) and divides the protoplasm into two separate subsequent daughter cells (Fig. 1H). The structural order of carbon in the cell plate is similar to that of the cell wall but higher (higher I-1350/1600) than that in the split protoplasm (Fig. 1H). During cytokinesis, the formation of two daughter nuclei is completed, and the protoplasm is gradually separated into two parts by the furrow (arrows) in the equator (Fig. 1F). A nucleolus with a smudged envelope is visible, in which the carbon is less ordered (lower I-1350/1600) than that in the nucleus matrix, whereas the carbon in cytoplasm has higher structural order (higher I-1350/1600) than that in the nucleus and cell wall (Fig. 1F).

4. Caption of Fig. DR1

Fig. DR1: Plots of all $\delta^{13}C_{org\text{-}SIMS}$ data obtained from both fossil and extant fern. The data on the left side of the dashed line (^{12}C count of sample vs. standard less than 7%) are excluded from our interpretation in order to avoid artifacts, as explained in the Methods section. The raw data are provided in Table DR. 1.

5. References of Data Repository

Bergelin, I., Obst, K., Söderlund, U., Larsson, K., and Johansson, L., 2011, Mesozoic rift magmatism in the North Sea region: $^{40}Ar/^{39}Ar$ geochronology of Scanian basalts and geochemical constraints: International Journal of Earth Sciences, v. 100, p. 787-804.

Bomfleur, B., McLoughlin, S., and Vajda, V., 2014, Fossilized nuclei and chromosomes reveal 180 million years of genomic stasis in royal ferns: Science, v. 343, p. 1376-1377.

McLoughlin**, S**. and Bomfleur,, B. 2016**.,** Biotic interactions in an exceptionally well preserved osmundaceous fern rhizome from the Early Jurassic of Sweden. Palaeogeography, Palaeoclimatology, Palaeoecology, v. 464*,* p. 86–96.

Morag, N., Williford, K.H., Kitajima, K., Philippot, P., Van Kranendonk, M.J., Lepot, K., Thomazo, C., Valley, J.W. (2016) Microstructure-specific carbon isotopic signatures of organic matter from ~3.5 Ga cherts of the Pilbara Craton support a biologic origin. Precambrian Research v. 275, p. 429-449.

Vajda, V., Linderson, H., and McLoughlin, S., 2016, Disrupted vegetation as a response to Jurassic volcanism in southern Sweden: Geological Society, London,

Special Publications, v. 434, p. 127-147.

Tappe, S., Smart, K.A., Stracke, A., Romer, R.L., Prelević, D., and van den Bogaard, P., 2016, Melt evolution beneath a rifted craton edge: 40 Ar/39 Ar geochronology and Sr–Nd–Hf–Pb isotope systematics of primitive alkaline basalts and lamprophyres from the SW Baltic Shield: Geochimica et Cosmochimica Acta, v. 173, p. 1-36.

Wacey, D., Kilburn, M.R., Saunders, M., Cliff, J., Brasier, M.D. (2011) Microfossils of sulfur-metabolizing cells in 3.4-billion-year-old rocks of Western Australia. Nature Geoscience v. 4, p. 698-702.

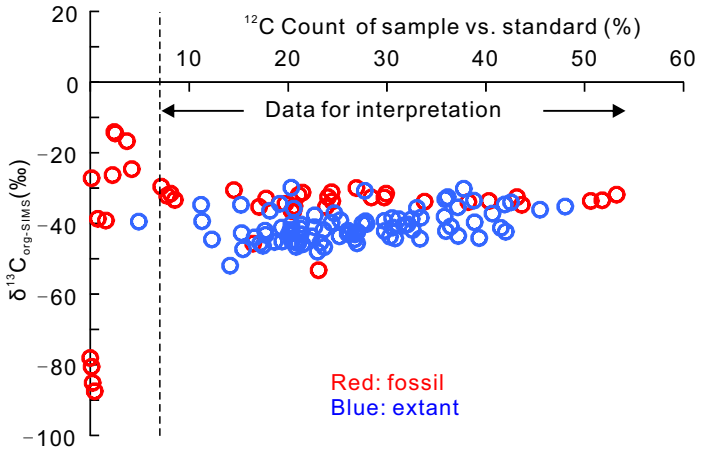
20
0
−20
−40
−60
−80
−100
δ13Corg-SIMS (‰)
12C Count of sample vs. standard (%)
10
20
30
40
50
60
Data for interpretation
Red: fossil
Blue: extant

Fig. DR1

Table DR1: Summary of $\delta^{13}C_{org–SIMS}$ data with count ratios. Abbreviations: RFF=Royal fern fossil, RFM=Royal fern modern, IP=Intensity of primary ion, cps=count per second. Classification: STD=Standard, 1=Cell wall in pith, 2=Nuclei in inner cortex, 3=Cytoplasm in inner cortex, 4=Cell wall in inner cortex, 5=Cytoplasm in outer cortex, 6=Cell wall in outer cortex. Note: some IP values (shown as blanks) were not recorded due to software problem. The underlines represent the data with ^{12}C counts of sample vs. STD <0.07, which are excluded from further consideration in order to avoid artifacts.

Sample ID	IP (nA)	^{12}C cps ($\times10^{9}$)	^{12}C cps sample vs. STD	$^{13}C/^{12}C$ drift corrected ($\times10^{-2}$)	± abs (10^{-5})	$\delta^{13}C$ (‰ in PDB)	Classification
0519@1	0.294	0.07		1.05	0.015	–30.65±0.28	STD
0519@2	0.293	0.07		1.05	0.013	–30.87±0.27	STD
0519@3	0.293	0.07		1.05	0.013	–31.21±0.27	STD
RFF_@1	0.292	0.02	0.24	1.05	0.026	–31.22±0.35	6
RFF_@02	0.291	0.01	0.21	1.05	0.034	–31.38±0.40	6
RFF_@03	0.290	0.03	0.40	1.04	0.022	–33.72±0.32	6
RFF_@04	0.289	0.03	0.38	1.04	0.023	–34.00±0.33	6
RFF_@05	0.288	0.03	0.43	1.04	0.019	–32.69±0.31	6
RFF_@06	0.287	0.03	0.51	1.04	0.025	–33.71±0.34	6
RFF_@07	0.286	0.00	0.02	1.04	0.113	–39.28±1.11	6
RFF_@08	0.286	0.01	0.21	1.05	0.030	–32.10±0.38	6

0519@4	0.285	0.07		1.05	0.015	–31.88±0.28	STD
0519@5	0.284	0.07		1.05	0.013	–31.13±0.27	STD
RFF_@09	0.284	0.02	0.24	1.04	0.026	–35.39±0.35	6
RFF_@10	0.283	0.01	0.09	1.04	0.044	–33.42±0.48	6
RFF_@11	0.282	0.00	0.00	1.62	2.572	503.46±24.58	2
RFF_@12	0.282	0.00	0.00	0.99	0.293	–87.59±2.81	2
RFF_@13	0.282	0.00	0.00	2.26	8.983	1089.53±85.85	2
RFF_@14	0.281	0.00	0.00	1.17	1.113	84.92±10.64	2
RFF_@15	0.281	0.00	0.00	1.73	5.180	601.96±49.50	2
RFF_@16	0.280	0.00	0.00	2.69	14.047	1494.30±134.24	2
0519@6	0.280	0.07		1.05	0.018	–30.55±0.30	STD
0519@7	0.280	0.07		1.05	0.013	–30.93±0.27	STD
RFF_@17	0.280	0.00	0.07	1.00	0.202	–78.24±1.95	4
RFF_@18	0.279	0.00	0.00	1.72	3.016	595.31±28.82	3
RFF_@19	0.279	0.01	0.17	1.03	0.041	–45.86±0.46	4
RFF_@20	0.278	0.00	0.02	1.05	0.093	–26.37±0.92	4
RFF_@21	0.278	0.01	0.18	1.04	0.033	–33.05±0.40	2
RFF_@22	0.278	0.03	0.52	1.04	0.018	–33.52±0.30	4
RFF_@23	0.278	0.00	0.00	0.99	0.340	–85.22±3.26	4
RFF_@24	0.278	0.03	0.44	1.04	0.019	–34.81±0.31	4
0519@8	0.277	0.07		1.05	0.014	–31.22±0.28	STD
0519@9	0.277	0.07		1.05	0.016	–31.08±0.29	STD
RFF_@25	0.277	0.00	0.00	0.99	1.073	–80.67±10.25	2

RFF_@26	0.277	0.00	0.00	1.59	3.653	472.10±34.91	2
RFF_@27	0.276	0.00	0.00	2.01	3.722	863.20±35.57	2
RFF_@28	0.276	0.00	0.00	1.62	1.225	500.15±11.71	2
RFF_@29	0.275	0.00	0.00	1.38	1.204	274.28±11.51	2
RFF_@30	0.275	0.00	0.00	1.22	2.062	131.19±19.71	2
RFF_@31	0.275	0.00	0.00	1.22	1.208	129.49±11.55	2
RFF_@32	0.274	0.00	0.00	1.05	0.617	–27.33±5.90	2
0519@10	0.274	0.06		1.05	0.018	–30.70±0.30	STD
0519@11	0.274	0.07		1.05	0.013	–31.07±0.27	STD
RFF_@33	0.273	0.00	0.00	1.35	2.646	245.94±25.29	2
RFF_@34	0.273	0.00	0.00	2.16	7.825	1004.41±74.78	2
RFF_@35	0.272	0.00	0.01	1.04	1.155	–38.82±11.04	2
RFF_@36	0.272	0.00	0.00	1.66	3.309	540.88±31.62	2
RFF_@37	0.272	0.00	0.07	0.93	0.442	–138.19±4.22	2
RFF_@38	0.271	0.00	0.00	2.25	9.515	1086.05±90.93	2
RFF_@39	0.271	0.00	0.00	1.48	5.309	374.66±50.73	2
RFF_@40	0.270	0.00	0.00	0.90	0.199	–166.92±1.92	2
0519@12	0.270	0.06		1.05	0.019	–31.40±0.30	STD
0519@13	0.269	0.06		1.05	0.018	–31.10±0.30	STD
RFF_@41	0.269	0.00	0.00	1.80	3.920	663.77±37.46	2
RFF_@42	0.268	0.00	0.00	1.85	6.100	711.99±58.29	2
RFF_@43	0.268	0.00	0.00	1.79	8.511	661.13±81.34	2
RFF_@44	0.267	0.00	0.00	3.12	15.334	1889.39±146.54	2

RFF_@45	0.267	0.01	0.21	1.04	0.029	–36.58±0.37	1
RFF_@46	0.267	0.01	0.20	1.04	0.030	–34.53±0.37	1
RFF_@47	0.266	0.01	0.15	1.05	0.035	–30.72±0.42	1
RFF_@48	0.266	0.01	0.17	1.04	0.032	–35.40±0.39	1
0519@14	0.266	0.06		1.05	0.013	–30.81±0.28	STD
0519@15	0.266	0.06		1.05	0.013	–31.26±0.27	STD
RFF_@49	0.265	0.01	0.21	1.04	0.032	–35.25±0.39	1
RFF_@50	0.265	0.01	0.23	1.02	0.069	–53.36±0.70	1
RFF_@51	0.265	0.02	0.24	1.04	0.027	–32.60±0.35	4
RFF_@52	0.264	0.02	0.25	1.04	0.026	–33.79±0.35	4
RFF_@53		0.02	0.34	1.04	0.023	–33.90±0.32	4
RFF_@54		0.03	0.53	1.05	0.018	–31.99±0.30	4
RFF_@55		0.00	0.04	1.06	0.071	–16.78±0.72	2
RFF_@56		0.02	0.27	1.05	0.027	–30.11±0.35	4
0519@16		0.08		1.05	0.013	–29.89±0.27	STD
0519@17		0.08		1.05	0.013	–30.66±0.28	STD
RFF_@57		0.00	0.03	1.06	0.096	–14.61±0.95	2
RFF_@58		0.02	0.28	1.04	0.026	–32.79±0.35	4
RFF_@59		0.00	0.04	1.05	0.061	–24.70±0.63	2
RFF_@60		0.02	0.30	1.05	0.026	–31.70±0.35	4
RFF_@61		0.01	0.07	1.05	0.044	–29.66±0.48	2
RFF_@62		0.01	0.08	1.05	0.042	–32.28±0.47	2
0519@18		0.08		1.05	0.016	–30.80±0.29	STD

0519@19	0.08		1.05	0.016	–30.87±0.29	STD
RFF_@63	0.02	0.30	1.04	0.026	–32.74±0.35	4
RFF_@64	0.00	0.02	1.06	0.092	–14.24±0.91	2
RFF_@65	0.01	0.08	1.05	0.042	–31.65±0.47	2
RFF_@66	0.02	0.20	1.04	0.034	–36.66±0.40	4
0519@20	0.08		1.05	0.017	–31.21±0.29	STD
0519@21	0.08		1.05	0.014	–31.14±0.28	STD
0520@1	0.07		1.05	0.018	–30.75±0.40	STD
0520@2	0.07		1.05	0.014	–31.51±0.39	STD
0520@3	0.07		1.05	0.013	–31.12±0.38	STD
RFM@1	0.00	0.00	–2.40	–1.751	–3213.74±16.68	1
RFM@02	0.00	0.05	1.04	0.057	–39.61±0.65	1
RFM@03	0.01	0.18	1.04	0.035	–42.20±0.49	1
RFM@04	0.02	0.23	1.04	0.026	–37.85±0.44	1
RFM@05	0.01	0.11	1.04	0.037	–39.45±0.51	1
RFM@06	0.01	0.11	1.05	0.038	–34.82±0.51	1
RFM@07	0.01	0.19	1.05	0.029	–34.57±0.45	1
RFM@08	0.02	0.27	1.04	0.025	–43.19±0.43	4
0520@4	0.07		1.05	0.013	–30.61±0.38	STD
0520@5	0.07		1.05	0.013	–30.76±0.38	STD
RFM@09	0.02	0.33	1.04	0.022	–44.46±0.42	4
RFM@10	0.03	0.39	1.04	0.020	–44.28±0.41	4

RFM@11	0.01	0.21	1.03	0.028	–46.71±0.45	4
RFM@12	0.02	0.31	1.04	0.028	–41.30±0.45	4
RFM@13	0.03	0.38	1.05	0.026	–30.23±0.44	4
RFM@14	0.01	0.12	1.04	0.036	–44.61±0.50	4
RFM@15	0.01	0.21	1.05	0.042	–35.93±0.54	4
0520@6	0.06		1.05	0.013	–30.65±0.39	STD
0520@7	0.07		1.05	0.013	–30.98±0.38	STD
RFM@16	0.01	0.20	1.05	0.028	–30.02±0.45	4
RFM@17	0.02	0.28	1.05	0.024	–30.84±0.43	4
RFM@18	0.01	0.15	1.05	0.035	–34.87±0.49	4
RFM@19	0.01	0.14	1.03	0.034	–52.06±0.48	4
RFM@20	0.02	0.25	1.04	0.026	–37.17±0.44	4
RFM@21	0.01	0.20	1.04	0.028	–41.96±0.45	4
RFM@22	0.03	0.46	1.05	0.025	–36.18±0.43	4
0520@8	0.07		1.05	0.013	–30.98±0.38	STD
0520@9	0.07		1.05	0.013	–31.47±0.38	STD
RFM@23	0.02	0.37	1.04	0.021	–43.60±0.41	4
RFM@24	0.02	0.36	1.04	0.026	–40.97±0.43	4
RFM@25	0.01	0.15	1.03	0.036	–47.37±0.49	4
RFM@26	0.01	0.17	1.04	0.031	–45.76±0.46	unknown
RFM@27	0.01	0.17	1.04	0.032	–44.05±0.47	unknown
RFM@28	0.01	0.18	1.04	0.032	–43.30±0.47	6
RFM@29	0.02	0.36	1.04	0.027	–38.22±0.44	5

RFM@30	0.01	0.21	1.03	0.029	–46.03±0.45	6
0520@10	0.07		1.05	0.017	–31.31±0.40	STD
0520@11	0.07		1.05	0.013	–31.53±0.38	STD
RFM@31	0.03	0.42	1.04	0.020	–41.34±0.41	5
RFM@32	0.01	0.19	1.04	0.030	–45.28±0.46	6
RFM@33	0.02	0.32	1.04	0.024	–40.71±0.43	5
RFM@34	0.02	0.33	1.04	0.022	–41.93±0.42	5
RFM@35	0.02	0.23	1.03	0.034	–48.12±0.48	6
RFM@36	0.02	0.28	1.04	0.027	–40.17±0.44	5
RFM@37	0.02	0.23	1.04	0.028	–45.64±0.45	6
RFM@38	0.03	0.43	1.05	0.020	–34.15±0.41	5
RFM@39	0.01	0.15	1.04	0.033	–42.89±0.48	6
0520@12	0.07		1.05	0.013	–30.84±0.38	STD
0520@13	0.07		1.05	0.013	–30.86±0.38	STD
RFM@40	0.02	0.25	1.04	0.036	–43.79±0.50	6
RFM@41	0.01	0.21	1.04	0.027	–43.16±0.44	5
RFM@42	0.01	0.19	1.04	0.029	–45.25±0.45	5
RFM@43	0.01	0.20	1.04	0.035	–45.11±0.49	6
RFM@44	0.03	0.48	1.05	0.018	–35.34±0.40	5
RFM@45	0.01	0.21	1.04	0.038	–45.71±0.51	6
RFM@46	0.02	0.27	1.04	0.032	–42.42±0.47	5
RFM@47	0.02	0.30	1.04	0.026	–42.22±0.44	5
RFM@48	0.02	0.26	1.04	0.025	–43.16±0.43	6

RFM@49	0.02	0.28	1.04	0.024	–40.27±0.43	5
0520@14	0.07		1.05	0.014	–30.48±0.39	STD
0520@15	0.07		1.05	0.013	–31.01±0.38	STD
RFM@50	0.01	0.20	1.04	0.028	–43.04±0.45	6
RFM@51	0.02	0.26	1.04	0.025	–42.92±0.43	5
RFM@52	0.02	0.26	1.04	0.032	–42.20±0.47	5
RFM@53	0.02	0.24	1.04	0.026	–41.96±0.44	6
RFM@54	0.03	0.42	1.04	0.023	–42.41±0.42	5
RFM@55	0.02	0.27	1.04	0.025	–44.51±0.43	6
RFM@56	0.02	0.22	1.04	0.034	–43.78±0.48	5
RFM@57	0.01	0.21	1.04	0.029	–45.32±0.45	6
0520@16	0.07		1.05	0.013	–31.07±0.38	STD
RFM@58	0.02	0.36	1.05	0.024	–33.27±0.43	5
RFM@59	0.02	0.24	1.04	0.035	–39.88±0.49	6
RFM@60	0.02	0.25	1.04	0.025	–39.17±0.43	5
RFM@61	0.02	0.33	1.04	0.031	–38.89±0.47	5
RFM@62	0.02	0.27	1.04	0.038	–45.69±0.51	6
RFM@63	0.03	0.39	1.04	0.021	–39.76±0.41	5
RFM@64	0.02	0.30	1.04	0.023	–39.43±0.42	6
RFM@65	0.02	0.33	1.05	0.022	–35.75±0.42	5
0520@18	0.07		1.05	0.013	–30.69±0.38	STD
0520@19	0.07		1.05	0.014	–30.95±0.39	STD
RFM@66	0.02	0.36	1.05	0.021	–32.66±0.42	5

RFM@67	0.03	0.42	1.05	0.020	–34.76±0.41	6
RFM@68	0.02	0.30	1.04	0.026	–43.84±0.43	5
RFM@69	0.01	0.19	1.04	0.031	–41.25±0.47	6
RFM@70	0.02	0.27	1.04	0.028	–43.05±0.45	5
RFM@71	0.02	0.31	1.04	0.023	–38.92±0.42	5
RFM@72	0.01	0.20	1.04	0.028	–42.39±0.45	6
RFM@73	0.02	0.28	1.04	0.024	–39.50±0.43	5
0520@20	0.07		1.05	0.013	–30.65±0.38	STD
0520@21	0.06		1.05	0.013	–31.83±0.38	STD
RFM@74	0.02	0.32	1.04	0.025	–40.33±0.43	5
RFM@75	0.01	0.20	1.04	0.032	–45.04±0.47	6
RFM@76	0.03	0.41	1.04	0.020	–37.33±0.41	5
RFM@77	0.02	0.24	1.03	0.035	–46.76±0.49	6
RFM@78	0.02	0.33	1.04	0.023	–38.50±0.42	5
RFM@79	0.02	0.31	1.04	0.026	–44.32±0.43	6
RFM@80	0.02	0.36	1.04	0.022	–42.22±0.41	5
RFM@81	0.02	0.37	1.05	0.021	–35.52±0.42	5
0520@22	0.07		1.05	0.014	–31.00±0.39	STD
0520@23	0.07		1.05	0.015	–31.24±0.39	STD
RFM@82	0.01	0.18	1.05	0.030	–36.51±0.46	1
RFM@83	0.01	0.18	1.03	0.030	–46.43±0.46	1
RFM@84	0.02	0.31	1.04	0.031	–38.56±0.47	1
RFM@85	0.01	0.21	1.04	0.028	–40.37±0.45	1

RFM@86	0.02	0.23	1.04	0.028	–41.12±0.45	1
RFM@87	0.03	0.39	1.05	0.021	–33.65±0.41	1
RFM@88	0.01	0.21	1.04	0.028	–41.43±0.45	1
RFM@89	0.01	0.20	1.04	0.028	–40.40±0.45	1
0520@24	0.07		1.05	0.013	–30.51±0.38	STD
0520@25	0.07		1.05	0.013	–31.22±0.38	STD

9

10